X-661-71-36



# CALIBRATION OF THE NASA-GSFC HIGH ENERGY COSMIC RAY EXPERIMENT

H. WHITESIDE
C. J. CRANNELL
H. CRANNELL
J. F. ORMES
M. J. RYAN

JANUARY 1971


GODDARD SPACE FLIGHT CENTER
GREENBELT, MARYLAND

# CALIBRATION OF THE NASA-GSFC

# HIGH ENERGY COSMIC RAY EXPERIMENT

Preliminary Report
January 1971

H. Whiteside
Federal City College

C. J. Crannell and H. Crannell
Catholic University of America

J. F. Ormes and M. J. Ryan
NASA/Goddard Space Flight Center

## Abstract

This report describes the experimental conditions under which the NASA-GSFC High Energy Cosmic Ray Experiment was calibrated with the G-10 + 4.7° test beam at the AGS at Brookhaven National Laboratory. A detailed discussion is given of the momentum of the test beam used. In addition, summaries of the data runs taken are included.

## I. The Problem

Cosmic rays are presently the subject of intensive study because of their relevance to the field of astrophysics. Astrophysics is concerned with the nature of extraterrestrial phenomena, especially with the nucleo-synthesis processes involved in building up the nuclear isotopes. Since primary cosmic rays bring us a sample of material from outside the solar system, a study of their charge, energy, and direction of arrival yields information on their formation and acceleration and on the properties of the interstellar medium through which they propagate.

Cosmic ray energies above $10^{15}$ eV have been studied mainly by means of extensive air showers, and energies below $10^{10}$ eV have been studied extensively using balloons and satellites. These studies have produced models of cosmic ray acceleration, propagation, and storage which can best be tested by studying the energy spectra and charge composition in the energy range $10^{10}$ to $10^{15}$ eV. At these energies the number of surviving primaries is too small relative to the secondary flux at sea level, or even at mountain altitudes. Therefore, experiments are being carried out at high altitudes (125,000 ft.) with equipment carried by research balloons, a method that allows the study of energies up to $10^{12}$ eV. Present experiments in the Soviet Union and planned experiments

in the United States use satellite-borne instruments to extend this energy range up to $10^{14}$ eV.

## II. The Instrument

An instrument to carry out the measurements described above has been designed and built at Goddard Space Flight Center by a group including J. F. Ormes, F. B. McDonald, and V. K. Balasubrahmanyan of the High Energy Astrophysics Branch.

This instrument contains four digitized spark chambers to define the trajectory of the incoming particle (see Figure 1). It also contains a charge-determining module consisting of two plastic scintillators that produce an output proportional to $Z^2/\beta^2$, a CsI(Tl) scintillator that produces an output proportional to $Z^2/\beta^2$, and a Cerenkov detector with an output proportional to $Z^2(1 - \frac{1}{\beta^2 n^2})$. Together, these four counters enable the determination of the charge Z of the incoming particle up to Z = 26, and they also provide triggers for the spark chamber system.

For energy measurement, an ionization spectrometer (IS) is used. This consists of alternate layers of high-Z absorber and plastic scintillator. Each scintillator section is viewed by a photo-multiplier tube which registers a pulse proportional to the number of particles traversing that section of the spectrometer. The cascade shower induced by the incoming particle results in many secondary particles. Measurement of the number of secondary particles at many points in the shower allows reconstruction of the energy of the incident particle. The top absorber layers are made of tungsten to study electrons by means of electromagnetic cascade showers, while the lower layers are made of iron to study incoming nucleons and nuclei by means of their nuclear cascade showers. The electron section contains 12 radiation lengths of tungsten, which is only 0.44 nuclear mean free paths. This is followed by up to 5.5 mean free

paths of iron in the nuclear cascade section.

The equipment uses one of four triggering modes, depending on the type of particle to be observed: electron mode, proton mode, heavy nuclei mode, and calibrate mode. The calibrate mode triggers on any particle within the aperture of the equipment, while the others are self-explanatory.

Physically, the ionization spectrometer weighs 3 tons. For flight purposes it is contained in a housing 5 feet in diameter by 8 feet long. The geometry factor for particles that traverse at least 3 mean free paths of material is about 600 $cm^2$ sr. The electronics readout time (dead time) is 0.05 sec, but the detector remains active only for 2 microseconds after passage of the first particle. The internal layout is shown in Figure 1.

## III. Calibration Requirements

In order to use the IS to measure particle energies, it is necessary to make a theoretical analysis of detector response as a function of energy. This will also be a function of arrival direction and particle type, and is best carried out using Monte Carlo techniques. Such calculations have been carried by V. Jones at Louisiana State University, and have influenced the design of the IS.

However, in order to make absolute energy measurements, the IS response must be calibrated using particles of known energy. This is necessary in order to determine the energy going into invisible processes such as nuclear excitation as well as the efficiency of various components in the system. Also, since the energy of each incoming particle is only sampled by the detector, the accuracy and resolution in these measurements depend on the fluctuations in the energy contained and energy lost by the IS. The distribution of these fluctuations must also be studied in the calibration run.

Since the instrument is designed for energy measurements in the range $10^{10}$ to $10^{14}$ eV, this calibration has been performed at the highest available machine energy. Lower energies were also used in order to allow a good check of the theory which is to be used to extrapolate to even higher energies. Because the fraction of the incident energy which escapes from the detector depends on the angle of incidence, the calibration has been carried out at several different angles. Calibration of the electron section has previously been accomplished using 5.4 to 18 GeV electrons at SLAC. Calibration of the nuclear section is the subject of this report. The data for this purpose were obtained using a proton beam at the AGS.

## IV. Physical Layout

The experiment was set up in the G-10 + 4.7° Test Beam[1,2,3] in the East Experimental Area at the AGS. The location was 2258 inches from $D_2$, approximately the same as the MIT-Brown Experiment (#416). The configuration of the beam transport system is given in Table I and illustrated in Figure 2. Because of power supply limitations, the maximum available momentum was about 20 GeV/c. Of the quadrupoles, only $Q_5$ and $Q_6$ were available during these runs. Power limitations prevented the use of $Q_2$, and the power supplies for the other quadrupoles had been removed. A brief description of the experimental apparatus in the beam upstream of our experiment is presented in Table II.

The IS was supported by jackscrews on a wheeled cart, allowing the horizontal position and orientation as well as the vertical position to be changed with respect to the incoming beam (see Figure 3).

The whole experiment was encased in a large light-tight tent to prevent light leakage into the photomultiplier tubes.

V. Data Acquired

The experiment arrived at BNL on 5 July, 1970 and was set up in a vertical position for test runs on cosmic ray muons. It was then moved into position in the beam and test runs conducted to set up triggering modes and the beam telescope during the period 13 - 17 July. The production runs were made from 18 July through 21 July. Following the production runs, a cosmic ray muon run was taken with the AGS off and the IS in the beam position. The experiment was removed from the beam and left BNL on 25 July, 1970.

Twenty four production runs of 5 to 10 thousand events each were made, as described in Table III. These runs will allow the study of the dependence of detector response on:

(1) Momentum ( from 10 to 20 GeV/c)

(2) Angle of Incidence (from 0° to 20°)

(3) Position of Incident Particle (various locations over the aperture, see Figure 4)

(4) Incident Particle (protons and pions)

(5) Depth of Spectrometer (3.5 to 5.5 nuclear mean free paths).

These measurements will allow the objectives listed in Section III above to be reached, with the exception that the highest momentum used was only 20 GeV/c rather than the desired 30 GeV/c.

VI. Triggering Requirements

Aside from triggering requirements which are internal to the IS itself, the following external requirements were established:

$B\ S_1\ S_2\ S_3\ \bar{N}\ \bar{C}$ for protons

$B\ S_1\ S_2\ S_3\ \bar{N}\ C$ for pions

B is a gate which is only open during the flat top of the beam spill. $S_1$ $S_2$ $S_3$ are scintillation counters in coincidence, forming a beam telescope as described in Table I. N is an anti-coincidence trigger fired by noise. C is a signal from the gas Cerenkov counter.

The anti-noise circuit was required to suppress noise pulses generated by the many spark chambers on the floor. A wire antenna a few feet long was used to pick up the noise, which was amplified (X10), sent through a discriminator, and finally to the anticoincidence gate.

The gas Cerenkov counter was filled to twice the threshold pressure for kaons at each beam momentum, a value which is about half the threshold pressure for protons. This allowed discrimination between protons and other particles such that at least 98% of all particles accepted when the Cerenkov is in anti-coincidence are protons.

Under these same conditions, but with the Cerenkov in coincidence, the + 10 GeV/c pion beam contains less than 9% kaon contamination. The + 20 GeV/c pion beam, however, requires a different setting of the gas pressure to get adequate discrimination against kaons, a procedure which was not followed in this particular experiment. The threshold pressures for various particles and momenta are listed in Table IV. The Cerenkov counter is built to operate at pressures up to 70 psia and above this pressure the safety valve will release.

## VII. Beam Momentum

One of the most difficult aspects in the analysis of this experiment is the determination of the central value of the beam momentum. Because the first collimator and the effective target position are not on the magnet axis, as shown in Figure 2, and because most of the focussing quadrupoles are not avail-

able for our range of beam momentum, the behaviour of the beam is far from ideal.

A. Momentum Resolution

In a beam transport system, momentum definition is accomplished by constraining the beam to lie along a line, to transit a particular bend angle, and to pass through a point. The momentum resolution is then determined by the angular resolution due to the finite width of the beam "line" and the aperture "point".

In this test beam the momentum resolution is determined by the angular resolution in the first bend angle as follows:

(1) The target $T_V$ and the exit aperture of the first collimator $C_1$ form a line with

$$\delta\,\theta = \frac{1.0}{268.25 + 18.0} = 3.50 \text{ mrad}$$

(2) The exit aperture of the second collimator $C_2$ forms a point with

$$\delta\,\theta = \frac{0.5}{460.75 + 24.0} = 1.03 \text{ mrad}$$

(3) Together this gives $\delta\,\theta_1 = 4.53$ mrad, which is the full width measured to the limiting rays. This is to be compared to the nominal bend angle $\theta_1 = 59.3$ mrad, thus

$$\frac{\delta\,\theta_1}{\theta_1} = \frac{4.53}{59.3} = 7.6\%$$

(4) If one assumes a transmission function of triangular shape (see below), then the full width at half maximum is half the width to the limiting rays, i.e., $\Delta\,\theta = 0.5\,\delta\,\theta$ and

$$\frac{\Delta\,p}{p} = \frac{\Delta\,\theta_1}{\theta_1} = 3.8\% \text{ FWHM}$$

This expected value for the resolution agrees closely with a value of $\frac{\Delta\,E}{E} = 4\%$ obtained directly using a lead glass detector at 8 GeV/c.[4]

If the variable collimator $C_3$ is closed to less than 0.58 inch width the resolution is somewhat improved. However, there was no monitor available for the width of $C_3$ during the experiment so the actual value cannot be calculated. Nevertheless it can be seen that at best, closing $C_3$ completely would give $\frac{\Delta p}{p}$ = 3% (FWHM).

As for the second bend, a similar analysis gives $\frac{\Delta \theta_2}{\theta_2}$ = 20%, which is obviously not the limiting aperture in this particular configuration. If better momentum resolution is desired, one can select only events which lie in a small area of the spark chamber in the NASA experiment. This is equivalent to using a narrower beam telescope after the second bending magnet, and could allow the resolution of the second bending system to become the limiting factor.

B. Tuning Procedure

The tuning procedure followed was similar to that used by previous groups:

(1) Set $D_2$ at the nominal value obtained by linear scaling from the 8 GeV/c MIT-Brown setup. (1300 amps corresponds to 8 GeV/c).

(2) Tune $D_1$ and $Q_5$ $Q_6$ for maximum flux in the beam telescope $S_1$ $S_2$ $S_3$.

(3) Close the variable collimator $C_3$ until about 100 particles/AGS pulse are obtained in $S_1$ $S_2$ $S_3$. Repeat (2) and (3) as necessary.

The difficulty arises when this method of tuning is followed because the momentum calculated directly from the current[5] in $D_1$ differs significantly from that calculated directly from the current in $D_2$, as shown in Table Va. Furthermore, the current required in $D_1$ is a strong function of the current in $Q_5$ $Q_6$, confirming that the beam is off-axis and considerable steering is being done by the quadrupoles.

C. Central Value of Beam Momentum

The momentum can be calculated from the magnet currents and the bend angle in either $D_1$ or $D_2$. However, the bend angle in the system associated with $D_1$ is uncertain because the beam coming from the target is off-axis (see Figure 2) and because an undetermined amount of steering is done by the quadrupoles $Q_5$ and $Q_6$. The bend angle in the $D_2$ system is also uncertain because of the large angular acceptance of the telescope $S_1$ $S_2$ $S_3$. The problem is to determine the beam momentum as accurately as possible in the face of these uncertainties.

Although the data were not recorded for this purpose, a further check on the momentum is provided by the proton thresholds on pressure curves taken with the gas Cerenkov counter. The momentum values obtained from the Cerenkov data are about 10% higher than the corrected values from the magnets, except at 10 GeV/c. However, the pressure curves are very steep near the threshold and they were measured in rather coarse steps, so the uncertainty is quite large in these determinations. Therefore, we rely on the magnets for momentum determination, and include the Cerenkov data merely for completeness. It would be possible in future experiments with this beam to use the Cerenkov counter specifically to determine the momentum, provided that the proton thresholds were measured within 1 psi or better. In the only instance where our measurements were of reasonable precision, at 10 GeV/c, the momentum from the Cerenkov agrees with that from the magnets as seen in Table Va.

D. Momentum from the $D_2$ System

In order to approach the evaluation of momentum from the $D_2$ magnet system, it is necessary first to consider the transmission properties of a beam telescope with apertures of unequal width. This is discussed in Appendix A. This background makes it possible to discuss the beam momentum in terms of the tuning procedures actually used.

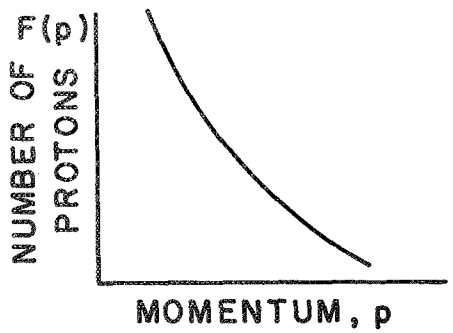


(1) It is known that the number of protons F(p) leaving the target along the beam line decreases rapidly with increasing proton momentum.[6] In fact, $\frac{d^2\sigma}{d\Omega dp} \sim p^{-5}$ or steeper in the region in question, so that $F(p) \sim p^{-4}$.

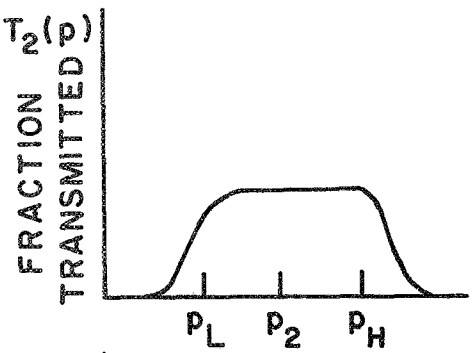


(2) It has been shown that the transmission function of the second magnet system has approximately trapezoidal shape centered about $p_2$, with $p_L$ and $p_H$ at the middle of the rounded shoulders. $p_2$ is the nominal momentum for which the current in $D_2$ is set.

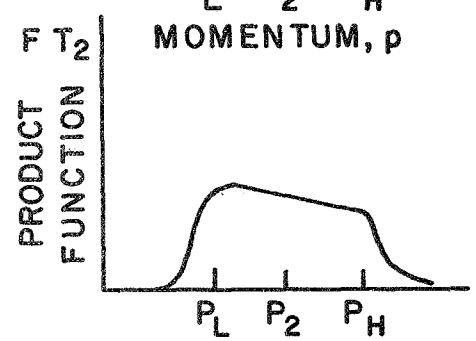


(3) When the production spectrum F(p) and the second bend transmission function $T_2(p)$ are folded together the result is a curve which is similar to a trapezoid with a tilted top.

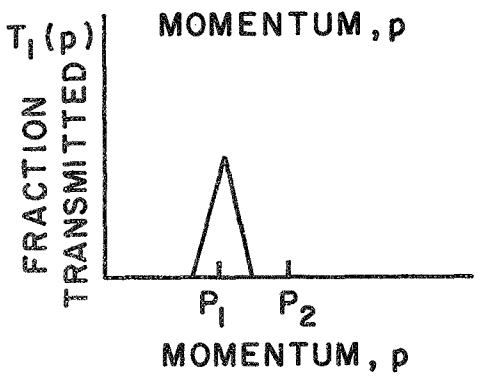


(4) The transmission function of the first magnet system has a narrow triangular shape. In tuning, the current in $D_1$ is adjusted for maximum flux, while $D_2$ is held fixed. That is, the integral $\int_0^\infty F(p)\ T_2(p)T_1(p)dp$ is maximized. A rough calculation indicates that the maximum occurs when $p_1 = p_L$, that is $T_1$ is centered at the lower shoulder of $T_2$. The uncertainty in this tuning is taken as $\pm \delta\theta_{c/2}$, i.e., the width of the rounded shoulder. For the particular system described here we then find

$$\frac{p_2 - p_1}{p_2} = \frac{1}{2}\left(\frac{\Delta p_2}{p_2}\right) = 10.1 \pm 2.2\%$$

Thus the actual beam momentum will be approximately 10.1% below the value corresponding to the current set in magnet $D_2$.

E. Momentum from the $D_1$ System

Another approach to the determination of beam momentum is to consider the situation at the first bending magnet. The bend angle at $D_1$ is nominally 59.3 mrad, but because of the fringe fields of the G-11 ring magnet the effective target point for positive beams lies outside the beam line. Also, the first collimator $C_1$ is displaced approximately 0.64 inches parallel to the beam line so that it defines an actual beam line somewhat different from the nominal one. The offset of the virtual target $T_V$ varies from 1.00 in at 20 GeV/c to 1.24 in at 10 GeV/c, which causes the required bend angle at $D_1$ to be 1.3 to 2.2 mrad greater than the nominal value. As a result, the actual momentum is expected to be 2.2% below the value calculated from the nominal bend angle at $D_1$ at 20 GeV/c and 3.7% below this value at 10 GeV/c, when the quadrupoles are off.

When the quadrupoles $Q_5$ & $Q_6$ are turned on, the tuned current in $D_1$ was found to be higher, so it is clear that some steering in opposition to the bend of $D_1$ is being done by the quads. From the 20 GeV/c data in Table VA, it is seen that this increase is about $\frac{2.5}{20.2}$ = 12% of the higher value when converted to momentum.

Since the source is off-axis, the beam enters $Q_5$ outside the axis and is bent towards the axis in the quads, which is in qualitative agreement with observations. Using the position of the first collimator (0.64 in outside the axis) and the focal length of the $Q_5Q_6$ pair (200 in) we estimate that a ray could be bent through $\frac{0.64}{200}$ = 3.2 mrad. This is to be compared with the nominal bend angle $\theta_1$ = 59.3 mrad, giving $\frac{3.2}{59.3}$ = 5.4%. Thus after turning the quads on we might expect to have to increase the current in $D_1$ by 5.4%. The fact that a larger increase is necessary suggests that our knowledge of the actual beam path prior

to $D_1$ remains ambiguous. This may be due to incomplete knowledge of the AGS fringing fields, or a misunderstanding as to the location of the off-axis components.

Using the experimentally determined value of 12% for the quadrupole steering and 2% for the off-axis location of $T_V$ we predict that the actual momentum is 14% below the value calculated from the current in $D_1$ at 20 GeV/c when the quads are on. Since data on the amount of steering done by $Q_5$ $Q_5$ are not available for lower momenta it is assumed that the same factor can be applied.

F. Combined Momentum Calculation

With the quads off, at nominal momentum 20 GeV/c, the momentum as calculated from $D_1$ is 17.65 GeV/c minus 2.6%, which gives 17.2 GeV/c. The analysis based on the bend at $D_2$ gives 19.8 GeV/c minus (10.1 $\pm$ 2.2)% which equals (17.8 $\pm$ 0.4)GeV/c. As our best value of the momentum, we quote the average, with error bars that encompass the full range of values within the uncertainties of either analysis alone. Thus the central value of beam momentum in this instance is (17.5 $\pm$ 0.7) GeV/c, or 17.5 GeV/c with an uncertainty of $\pm$ 4%.

With the quads on, at nominal momentum 20 GeV/c, the momentum as calculated from $D_1$ would then be 20.1 GeV/c minus 14%, which gives 17.3 GeV/c. The analysis based on the bend at $D_2$ gives 19.8 GeV/c minus (10.1 $\pm$ 2.2)% which equals (17.8 $\pm$ 0.4) GeV/c. Combining as before gives a central value of beam momentum of (17.55 $\pm$ 0.65) GeV/c, or 17.6 GeV/c with an uncertainty of $\pm$ 4%. This procedure is used in calculating the beam momentum in all experimental runs with the quads on. The results of the calculations are presented in Table Va.

Table Vb then gives the central value of beam momentum for each data run. These values are uncertain by $\pm$ 4%. The resolution of the momentum distribution is, coincidentally, 4% FWHM as discussed in Section VII A above.

VIII. Acknowledgements

Thanks are extended to R. Lanou and L. Rosenson of the MIT-Brown Group for the use of the Cerenkov counter, and S. Siegler for the use of the beam telescope. We especially want to thank R. Kurz for providing us with the very useful report[7] of his BNL calibration. Thanks are also extended to J. Tanguay and the entire crew at the AGS, who assisted in many ways. Appreciation is also expressed to the several other experimenters with whom we shared the Test Beam.

Several students participated in the data runs in addition to the authors of this report. These include: R. Silverberg of Goddard Space Flight Center, A. Peterson and D. Dellatorre of Catholic University of America, and R. Cunningham, J. Reynolds, and S. Withers of Federal City College.

Finally, a special word of appreciation is in order for the technical staff from Goddard Space Flight Center, including L. Stonebraker, J. Laws, M. Powers, and R. Greer, all of whom put in many long hours ensuring that the experiment would operate properly.

APPENDIX A

## Transmission of a Beam Telescope

A beam telescope which has apertures of unequal width is shown below:

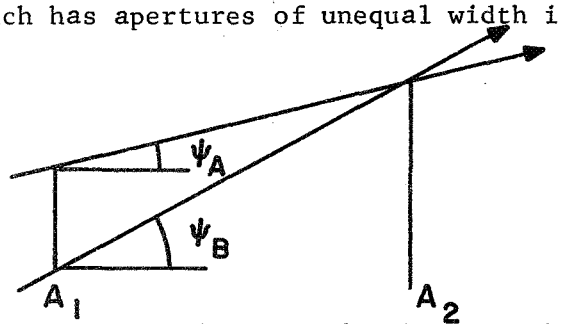


All rays which pass through aperture $A_1$ at angles between the axis (zero degrees) and $\pm \psi_A$ are transmitted, so the transmission function in this region is a constant, $T_0$. No rays pass through which travel at angles greater than $\psi_B$ with the axis, so that the transmission function drops to zero at $\pm \psi_B$. Finally, at angles between $\psi_A$ and $\psi_B$ there is a linear fall-off in the transmission function. Altogether this leads to a trapezoidal transmission function for the telescope, as shown below. In the special case where the apertures are equal, $\psi_A = 0$ and T ($\psi$) reduces to a triangular shape.

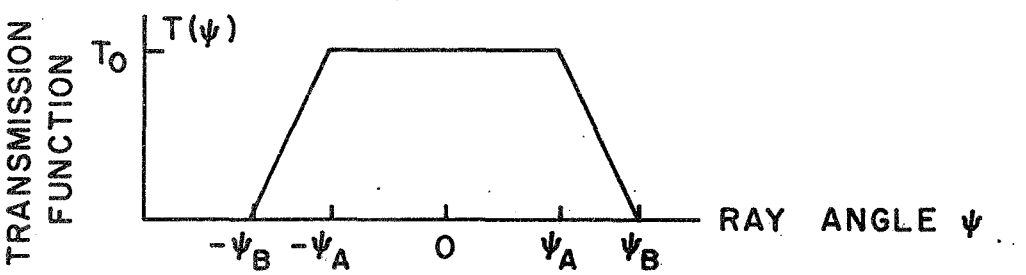


When a beam telescope is combined with a momentum-defining system, the transmission as a function of angle with respect to the beam axis is equal to the transmission as a function of the bend angle for rays constrained to pass through a point source. If the point source is replaced by a finite aperture, the transmission as a function of bend angle, T ($\theta$), is modified. The corners are rounded and the limiting angles of the "trapezoid" become larger as shown below. This effect is confined to a region within $\pm \delta\theta_c/2$ of the corners, where $\delta\theta_c$ is the full angular width of the aperture in question.

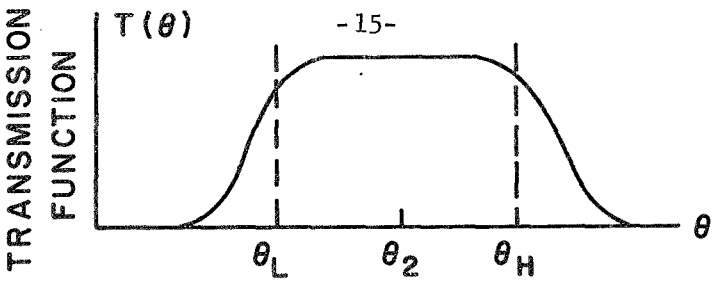


Therefore, the transmission function of the second bend system in the test beam discussed here is determined as follows:

(1) The scintillators $S_1$ and $S_2$ form a beam telescope with angles

$$\psi_A = \frac{4 - 1}{2\ (612)} = 2.45 \text{ mrad}$$

$$\psi_B = \frac{4 + 1}{2\ (612)} = 4.07 \text{ mrad}$$

(2) The entrance aperture of the second collimator $C_2$ approximates a point with angular width

$$\delta\ \theta_c = \frac{0.5}{950.5 - (460.75 - 24.0)} = 1.07 \text{ mrad}$$

(3) The shoulders of the transmission curve occur at $\theta_L = \theta_2 - \psi_A$ and $\theta_H = \theta_2 + \psi_A$. Therefore, the telescope has a full width to the shoulders of

$$\delta\ \theta_2 = 2\ \psi_A = 4.9 \text{ mrad}$$

This is to be compared to the nominal bend angle $\theta_2 = 24.2$ mrad, and converted to momentum, thus:

$$\frac{\Delta\ p_2}{p_2} = \frac{p_H - p_L}{p_2} = \frac{\theta_H - \theta_L}{\theta_2} = \frac{4.9}{24.2} = 20\% \text{ (Full Width to Shoulders)}$$

(4) The shoulders of the transmission curve are smeared out by $\pm \frac{\delta\ \theta_c}{2} = \pm\ 0.54$ mrad $= \pm\ 2.2\%$ due to the finite aperture of the collimator $C_2$.

APPENDIX B

## Preliminary Results

The figures presented in this Appendix are produced from computer printout showing a preliminary analysis of typical calibration runs made with 20, 15, and 10 GeV protons. The events included were selected to have interacted in one of the first 4 iron modules (2 interaction lengths). Figures B1 through B3 show the total number of particles, normalized to a mean of 100, detected in the first 7 iron modules (3-1/2 interaction lengths), for 20, 15, and 10 GeV incident protons respectively.

Figures B4 through B6 show the number of particles, normalized to a mean of 100, detected at cascade maximum for 20, 15, and 10 GeV protons respectively.

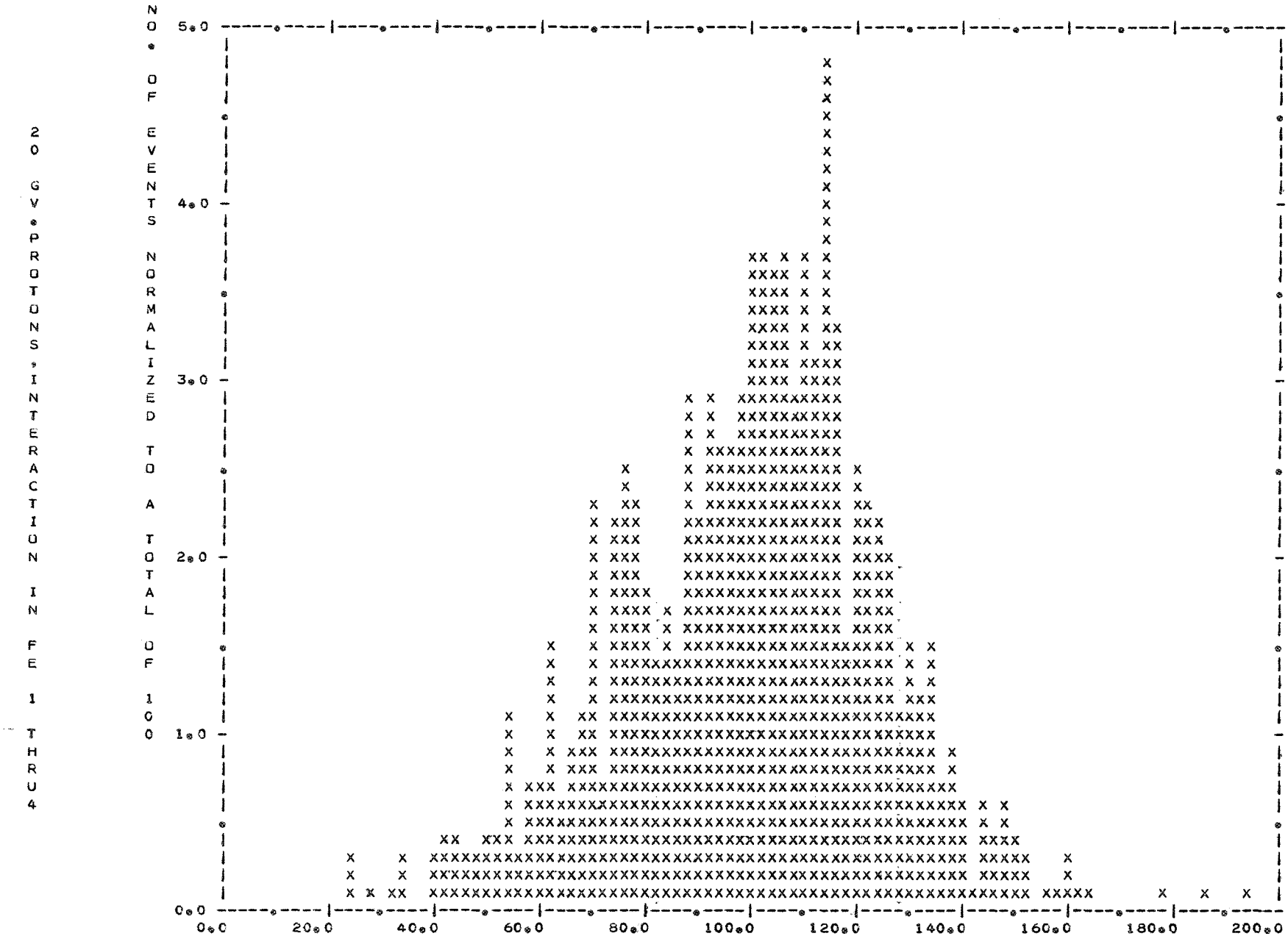


20 GV. PROTONS, INTERACTION IN FE 1 THRU 4

MEAN = 79.4 MODAL = 90.5 MEDIAN = 81.8 TOTAL NO. OF EVENTS = 635

STANDARD DEVIATION = 20.03 =25.24%

NEGATIVE STANDARD DEVIATION = 21.42 = 27.0% 294 EVENTS

POSITIVE STANDARD DEVIATION = 18.79 = 23.7% 341 EVENTS

FIGURE B1

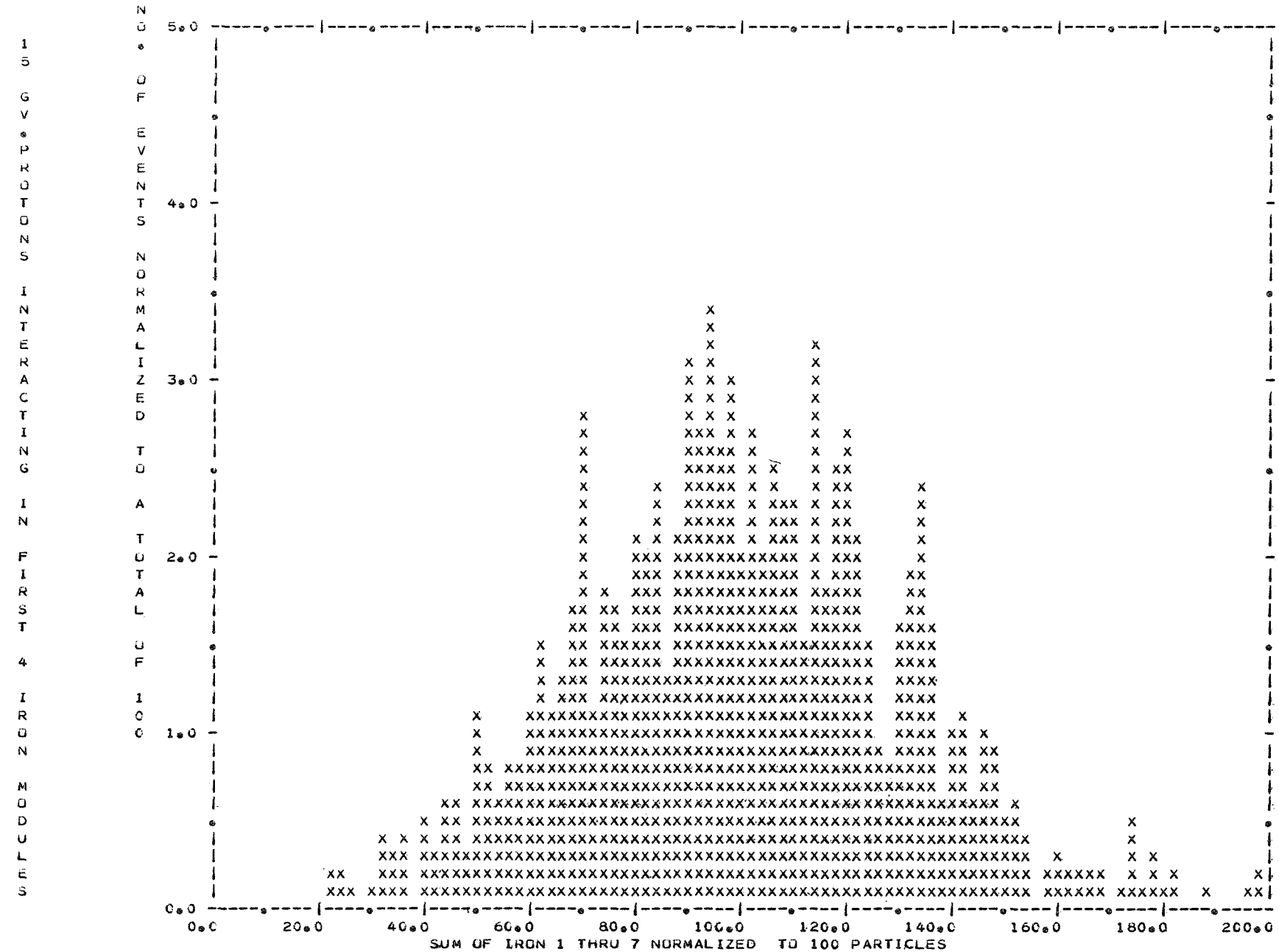


MEAN = 53.0 MODAL = 54.6 MEDIAN = 57.5 TOTAL NO.OF EVENTS = 866
STANDARD DEVIATION = 17.90 =30.84%
NEGATIVE STANDARD DEVIATION = 17.38 = 29.9% 443 EVENTS
POSITIVE STANDARD DEVIATION = 18.45 = 31.8% 423 EVENTS

FIGURE B2

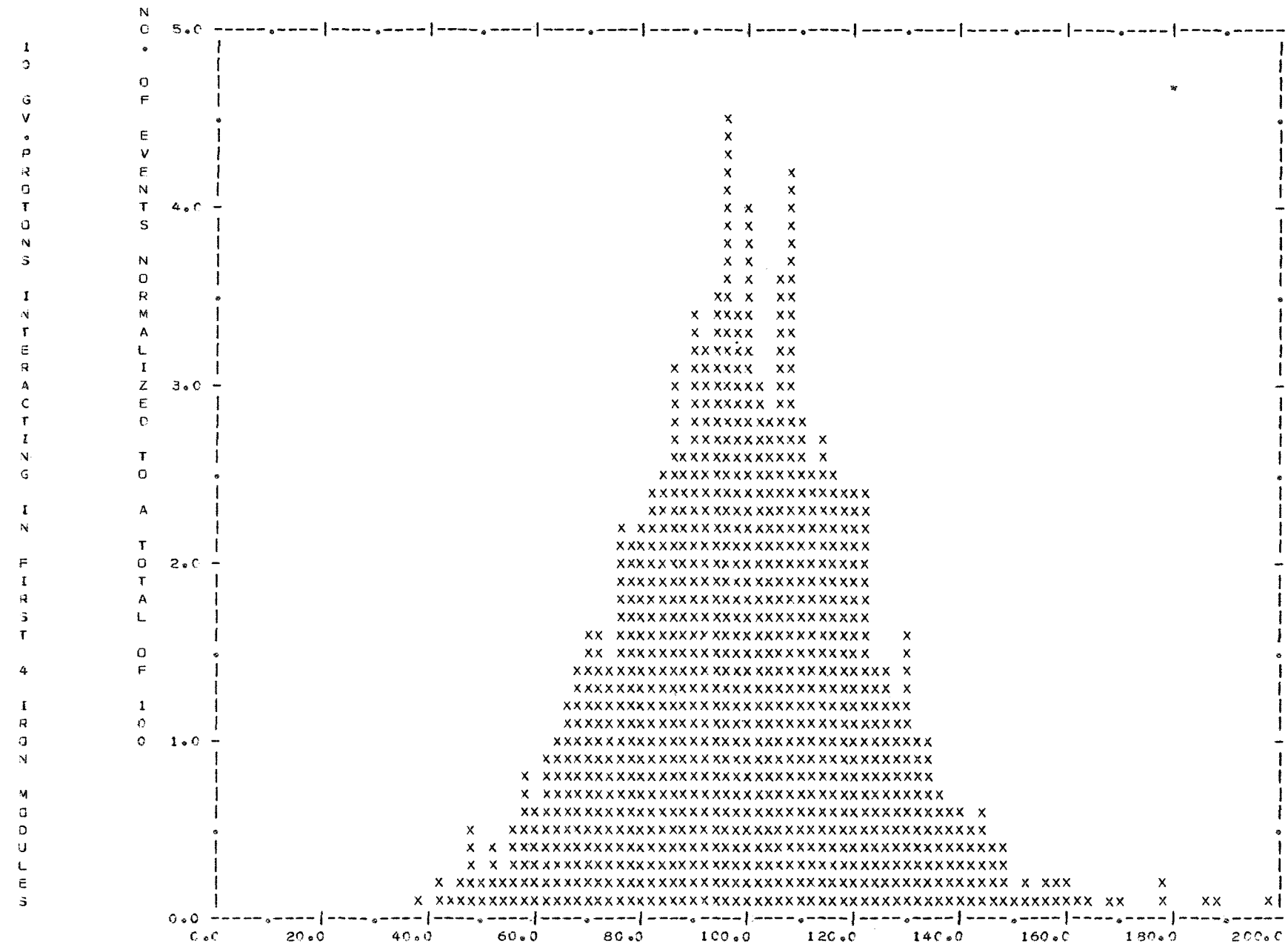


MEAN = 48.6 MODAL = 46.6 MEDIAN = 49.0 TOTAL NO.OF EVENTS = 1490
STANDARD DEVIATION = 11.73 =24.15%
NEGATIVE STANDARD DEVIATION = 11.01 = 22.7% 768 EVENTS
POSITIVE STANDARD DEVIATION = 12.46 = 25.7% 722 EVENTS

FIGURE B3

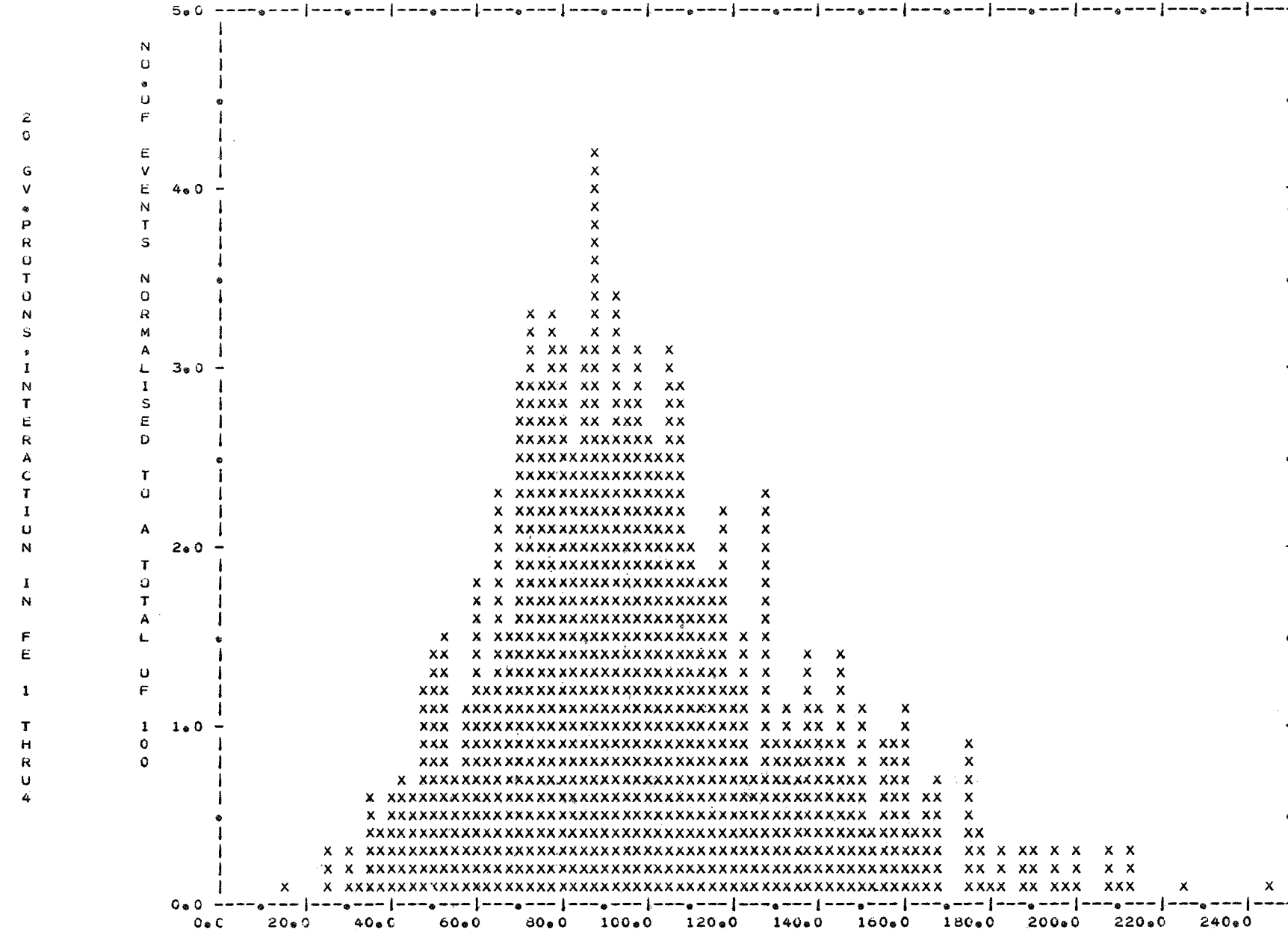


MEAN = 31.1 MODAL = 27.2 MEDIAN = 29.9 TOTAL NO.OF EVENTS = 635
STANDARD DEVIATION = 11.34 =36.46%
NEGATIVE STANDARD DEVIATION = 9.49 = 30.5% 360 EVENTS
PUSITIVE STANDARD DEVIATION = 13.39 = 43.1% 275 EVENTS

FIGURE B4

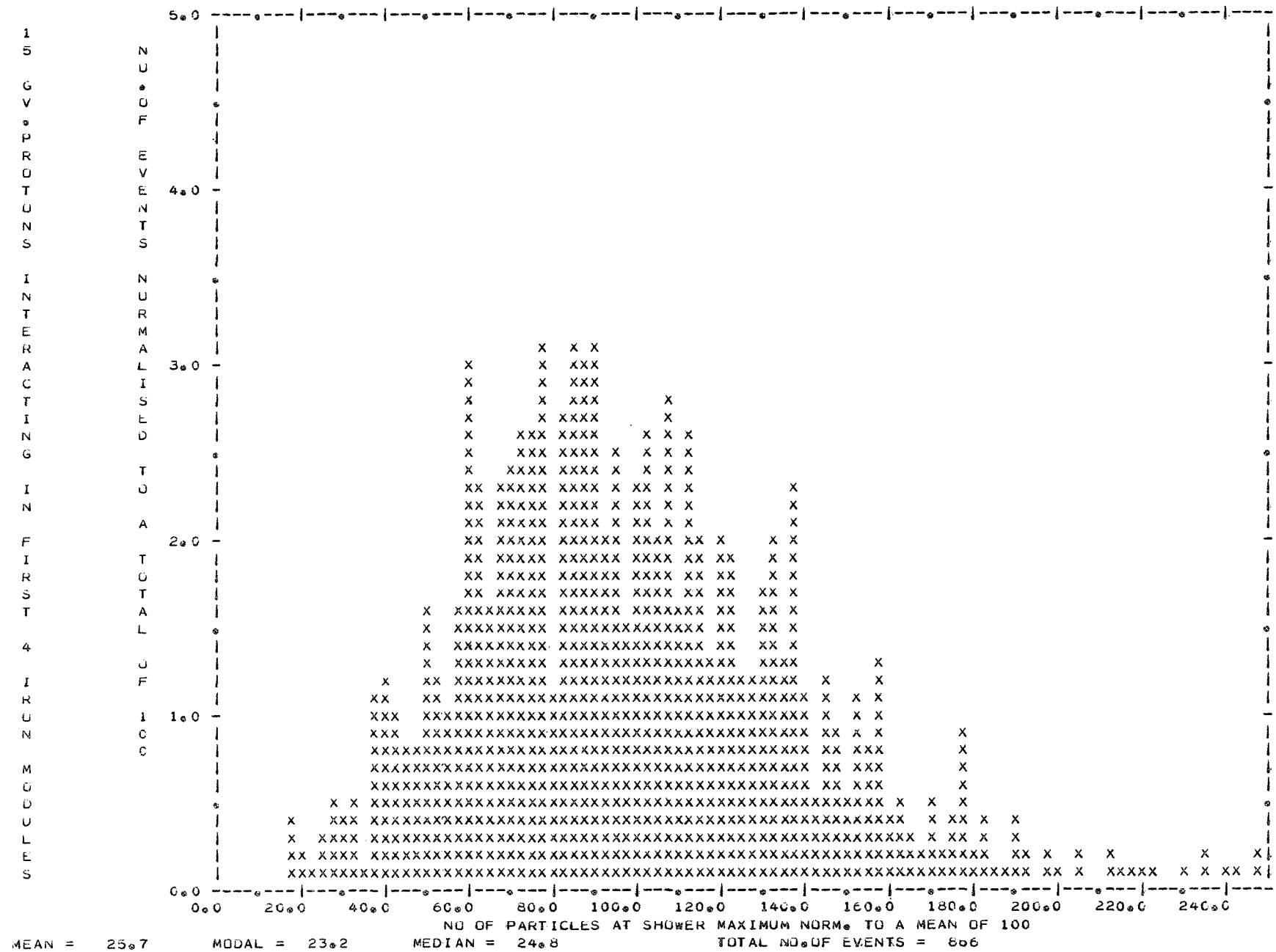


MEAN = 25.7 MODAL = 23.2 MEDIAN = 24.8 TOTAL NO. OF EVENTS = 866

STANDARD DEVIATION = 10.57 =41.03%

NEGATIVE STANDARD DEVIATION = 9.11 = 35.4% 470 EVENTS

POSITIVE STANDARD DEVIATION = 12.08 = 46.9% 396 EVENTS

FIGURE B5

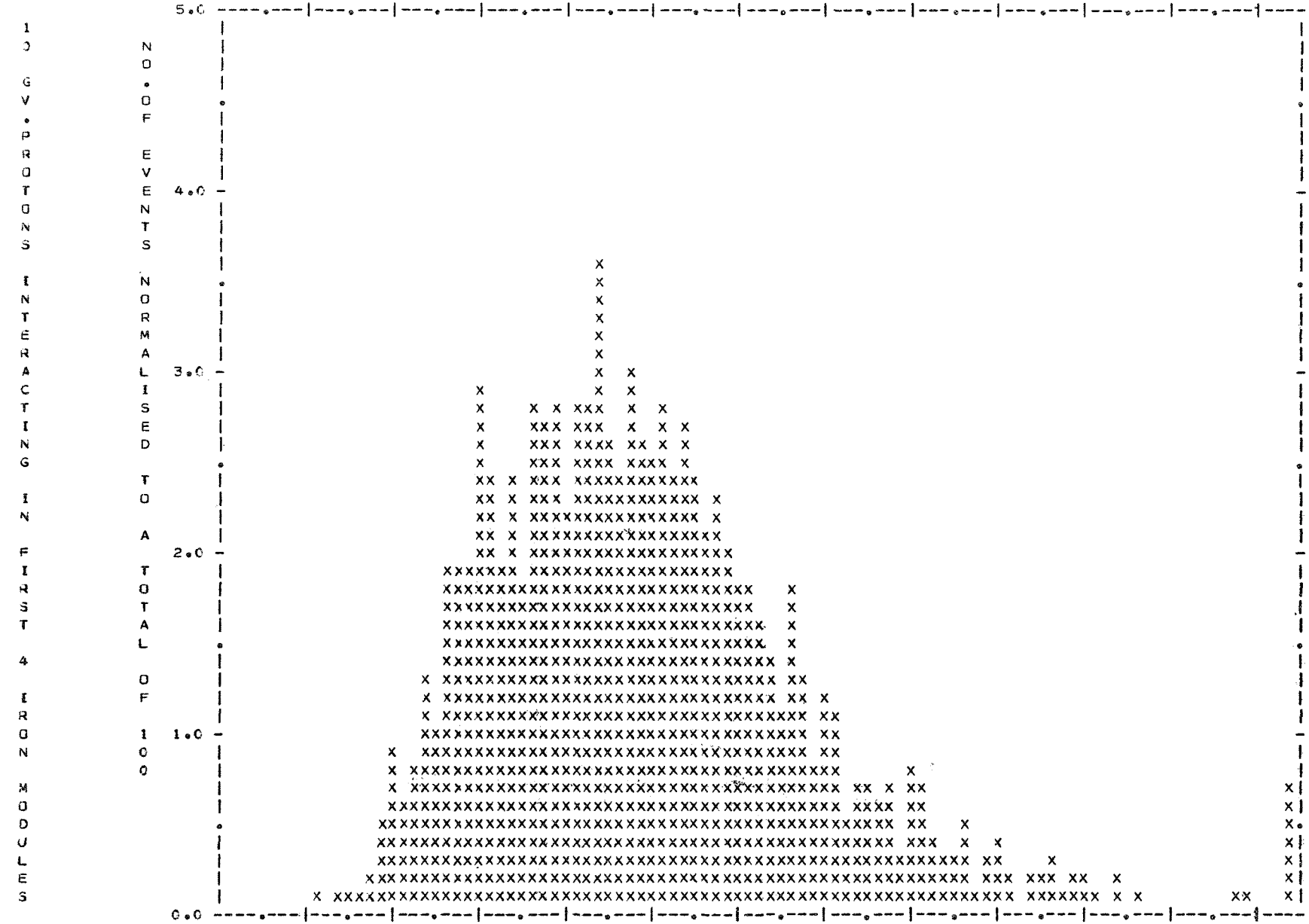


MEAN = 20.2 MODAL = 17.6 MEDIAN = 19.4 TOTAL NO.OF EVENTS = 1490
STANDARD DEVIATION = 7.89 =39.13%
NEGATIVE STANDARD DEVIATION = 6.37 = 31.6% 833 EVENTS
POSITIVE STANDARD DEVIATION = 9.47 = 47.0% 657 EVENTS

FIGURE B6

REFERENCES

(1) The beam is described in BNL E P & S Division Technical Note No. 2, A. L. Read, March 10, 1967.

(2) An earlier version of the beam is described in BNL 9213, A. L. Read and R. Rubenstein, ca. 1964.

(3) The beam layout for the MIT-Brown experiment is shown in BNL drawings D14-387 of 13 Jan. 1969 and D14-421 of 21 Oct. 1969.

(4) S. Siegler, private communication.

(5) The momentum calculations are based on the magnet data given in BNL Accelerator Department Internal Report GTD-2, Gordon T. Danby, 26 Dec. 1961.

(6) D. Dekkers et al., Phys. Rev. 137, B962 (1965) and R. A. Lundy et al., Phys. Rev. Letters 14, 504 (1965).

(7) R. J. Kurz, CRISP Calibration Experiment, NASA-MSFC Technical Note 33, (1970).

(8) The target is described in BNL E P & S Division Technical Note No. 22, G. E. Tanguay, December 16, 1968.

## LIST OF TABLES

TABLE I

LAYOUT OF G-10 + 4.7° TEST BEAM, 18-21 July, 1970

| Element | Symbol | Location | Description |
|---|---|---|---|
| G-10 Target | T | Between G-10 & G-11 ring magnets | BeO wire, described in Reference (8) |
| Virtual Target | $T_V$ | On a radial line through G10 target | BeO wire, offset by fringe field of G11 |
| Collimator #1 | $C_1$ | 268.25" from T | 1" hor x 4" vert x 36" lead |
| Quadrupole #5 | $Q_5$ | 563" from T on "magnet axis" | Type 8Q48 |
| Quadrupole #6 | $Q_6$ | 623" from T on "magnet axis" | Type 8Q48 |
| Bending Magnet #1 | $D_1$ | 701" from T | Type 18D72 - bend angle 3.4025° w.r.t. "magnet axis" |
| Collimator #2 | $C_2$ | 460.75" from $D_1$ | 1/2" x 1/2" x 48" lead, with brass shims |
| Collimator #3 | $C_3$ | 535.75" from $D_1$ | Variable width x 4" vert. x 48" lead automatic collimator |
| Bending Magnet #2 | $D_2$ | 950.5" from $D_1$ | type 18D72 - bend angle 1.3916° |
| Scint. Counter #1 | $S_1$ | 500" from $D_2$ (Nominal) | 4" wide x 3-1/2" high plastic |
| Cerenkov Counter | C | 549" from $D_2$ (to entrance) | 2 meter long gas Cerenkov counter |
| Scint. Counter #2 | $S_2$ | 612" from $S_1$ | 1" x 1" plastic |
| Scint. Counter #3 | $S_3$ | 55" from $S_2$ | 2" x 2" plastic |
| NASA Experiment | IS | 2258" from $D_2$ | Ionization Spectrometer |

TABLE II

OTHER EXPERIMENTS IN BEAM

| | |
|---|---|
| Rutgers (Maglic) | Scintillators $\sim$ 4 gm-cm$^{-2}$ |
| SUNY (Good) | ---- |
| Rockefeller (Cool) | Scintillators $\sim$ 1 gm-cm$^{-2}$<br>Gas Cerenkov Counter $\sim$ 1 gm-cm$^{-2}$ |
| Yale (Marx) | Scintillators $\sim$ 4 gm-cm$^{-2}$ |
| BNL (Collins) | Spark Chambers only |
| Columbia - NAL - Rochester<br>(Limon - White - Melissinos) | Scintillators $\sim$ 5 gm-cm$^{-2}$<br><br>Spark Chambers<br>18 layers of 4 mil<br>Aluminized Mylar<br><br>18 wire planes of 4 or 5 mil<br>Beryllium-Copper spaced 16/cm |

TABLE III. LIST OF CALIBRATION RUNS

| BNL Tape | ANALOG Track | PARTICLE | MOMENTUM GeV/c | INCIDENT ANGLE | POSITION | REF. TO DATABOOK & REMARKS | BNL Tape | DIGITAL File | BNL Tape | ANALYSIS File |
|---|---|---|---|---|---|---|---|---|---|---|
| | | | | | (SEVEN IRON MODULES) | | | | | |
| | PRELIMINARY SETUP RUNS | | | | | | | | | |
| | | | | | | First 2 Min. | | | | |
| 1 | 1 | $\mu$ | | | | (60,63)were rewritten | 1 | 1 | | |
| 1 | 4 | P & $\pi^+$ | 10 | 0° | 1 | (63) | 2 | 2 | 1 | 2 |
| 1 | 7 | P | 10 | 0° | 1 | (66) | 2 | 1 | 1 | 1 |
| 2 | 1 | P & $\pi^+$ | 20 | 0° | 1 | (67, 68) | 6 | 1 | 1 | 6 |
| 2 | 4 | P | 20 | 0° | 1 | (74) | 7 | 1 | 1 | 7 |
| 2 | 7 | P | 20 | 0° | 1 | (77) | 8 | 1 | 1 | 8 |
| 3 | 1 | P | 15 | 0° | 1 | (80) | 4 | 1 | 1 | 4 |
| | 0000 SATURDAY, 18 JULY 1970 | | | | | | | | | |
| 3 | 4 | P | 20 | 0° | 1 | (87) | 3 | 1 | 1 | 3 |
| 3 | 7 | P | 15 | 0° | 1 | (88) | 5 | 1 | 1 | 5 |
| 4 | 1 | P | 15 | 0° | 1 | (92) | 9 | 1 | 1 | 9 |
| 4 | 4 | P | 15 | 13° | 1 | (95) | 10 | 1 | 1 | 10 |
| 4 | 7 | P | 20 | 13° | 1 | (97) | 11 | 1 | 1 | 11 |
| 5 | 1 | P | 10 | 13° | 1 | (100) | 12 | 1 | 1 | 12 |
| | 0000 SUNDAY, 19 JULY 1970 | | | | | | | | | |
| 5 | 4 | P | 20 | 20° | 1 | (103) | 13 | 1 | 1 | 13 |
| 5 | 7 | P | 10 | 20° | 1 | (104) | 14 | 1 | 1 | 14 |
| 6 | 1 | P | 10 | 20° | 5 | (105) | 15 | 1 | 1 | 15 |
| 6 | 4 | P | 10 | 0° | 1 | (106) | 16 | 1 | 1 | 16 |
| 6 | 7 | $\pi^+$ | 10 | 0° | 1 | (107) | 17 | 1 | 1 | 17 |
| 7 | 1 | P | 10 | 0° | 2 | (111) | 18 | 1 | 1 | 18 |
| 7 | 4 | P | 10 | 0° | 3 | (112) | 19 | 1 | 1 | 19 |
| 7 | 7 | P | 10 | 0° | 4 | (113) | 20 | 1 | 1 | 20 |

TABLE III. (CONTINUED)

| BNL Tape | ANALOG Track | PARTICLE | MOMENTUM GeV/c | INCIDENT ANGLE | POSITION | REF. TO DATABOOK & REMARKS | BNL Tape | DIGITAL File | BNL Tape | ANALYSIS File |
|---|---|---|---|---|---|---|---|---|---|---|
| 0000 MONDAY, 20 JULY 1970 | | | | | | | | | | |
| 8 | 1 | P | 20 | 0° | 4 | (117) | 21 | 1 | 1 | 21 |
| 8 | 4 | P | 20 | 0° | 3 | (121) | 22 | 1 | 1 | 22 |
| 8 | 4 | P | 20 | 0° | 3 | (121) | 23 | 1 | 2 | 1 |
| 8 | 7 | P | 20 | 0° | 2 | (122) | 24 | 1 | 2 | 2 |
| 9 | 1 | P | 20 | 0° | 1 | (125) | 25 | 1 | 2 | 3 |
| 9 | 4 | P | 20 | 0° | 1 | (125) | 26 | 1 | 2 | 4 |
| 0000 TUESDAY, 21 JULY 1970 | | | | | | (FOUR IRON MODULES ADDED) | | | | |
| 9 | 7 | P | 20 | 0° | 1 | (131) Q5 & 6 Off | 27 | 1 | 2 | 5 |
| 10 | 1 | P | 20 | 0° | 1 | (133) | 28 | 1 | 2 | 6 |
| 10 | 4 | P | 20 | 18° | NECK | (136) | 29 | 1 | 2 | 7 |
| 10 | 7 | P | 20 | 18° | 1 | (137) | 30 | 1 | 2 | 8 |
| 11 | 1 | $\pi^+$ | 20 | 0° | 1 | (138) | 31 | 1 | 2 | 9 |
| 11 | 4 | $\pi^+$ | 20 | 0° | 1 | (138) | 32 | 1 | 2 | 10 |
| 11 | 7 | | | | | DOESN'T EXIST | | | | |
| CALIBRATION RUNS WITH AGS OFF (ALMOST) | | | | | | | | | | |
| 12 | 1 | $\mu$ | | | | (139) | 34 | 1 | 3 | 3 |
| 12 | 4 | $\mu$ | | | | COINCIDENCE DEMANDED | 35 | 1 | 3 | 4 |
| 12 | 7 | $\mu$ | | | | BETWEEN S1 & Fe4 or Fe7 | 36 | 1 | 3 | 5 |
| 13 | 1 | $\mu$ | | | | | 37 | 1 | 3 | 1 |
| 13 | 4 | $\mu$ | | | | DETECTOR STILL ON ITS SIDE | 38 | 1 | 3 | 2 |

TABLE IV

Threshold Pressures for Cerenkov Counter
Filled with Freon - 12 ($CCl_2F_2$)

(Calculated from $n_{threshold} = 1/\beta$, and using Argonne National Laboratory Report #6916, "Index and Dispersion of Cerenkov Counter Gases")

| | PARTICLE | | |
|---|---|---|---|
| MOMENTUM | PROTON | K | $\pi$ |
| 5 GeV/c | (550) | 70 | 4.8 |
| 10 GeV/c | 52 | 17 | 1.4 |
| 15 GeV/c | 27 | 8 | 0.6 |
| 20 GeV/c | 16 | 5 | 0.3 |

All pressures in psia

TABLE Va

TUNING RUN[2] MOMENTA (GeV/c)

| Momentum (Nominal) | Page In Log | DVM READINGS $D_2$ | DVM READINGS $D_1$ | DVM READINGS $Q_5$ $Q_6$ | RAW MOMENTUM from $D_2$ | RAW MOMENTUM from $D_1$ | CORRECTED MOMENTUM[1] from Cerenkov | CORRECTED MOMENTUM[1] from $D_2$ | CORRECTED MOMENTUM[1] from $D_1$ | CORRECTED MOMENTUM[1] Combined value |
|---|---|---|---|---|---|---|---|---|---|---|
| 20 | 73 | 57.5 ($Q_2$ = 49.1) | 57.0 | 39.0 | 19.8 | 20.0 | | 17.8 | -- | -- |
| | 117 | 57.5 | 57.1 | 36.1 | 19.8 | 20.1 | | 17.8 | 17.4 | 17.6 |
| | 130 | 57.5 | 56.6 | 30.0 | 19.8 | 19.9 | 18.9 ± 1.3 | 17.8 | 17.2 | 17.5 |
| | 133 | 57.5 | 57.5 | 37.0 | 19.8 | 20.5 | | 17.8 | 17.7 | 17.75 |
| 20 | 116 | 57.5 | 48.3 | off | 19.8 | 17.7 | | 17.8 | 17.3 | 17.55 |
| | 129 | 57.5 | 48.0 | off | 19.8 | 17.6 | | 17.8 | 17.2 | 17.5 |
| 16.5 | 67 | 47.5 (tuned $D_2$, not $D_1$) | 49.1 | 29.0 | 16.5 | 17.9 | | 14.8 | 15.4 | 15.1 |
| 15 | 89 | 44.2 | 43.0 | 33.0 | 15.2 | 15.9 | | 13.6 | 13.7 | 13.65 |
| | 86 | 44.2 | 42.5 | 32.8 | 15.2 | 16.0 | 14.9 ± 0.7 | 13.6 | 13.8 | 13.7 |
| | 91 | 44.2 | 43.7 | 37.1 | 15.2 | 16.2 | | 13.6 | 14.0 | 13.8 |
| 10 | 104 | 29.4 | 29.1 | 26.5 | 10.2 | 10.85 | | 9.2 | 9.4 | 9.3 |
| | 44 | 29.4 ($Q_2$ = 49.0) | 25.1 | 21.0 | 10.2 | 9.5 | 9.3 ± 0.2 | 9.2 | -- | -- |

(1) The momentum calculation is described in the text. The central value is known to about 4%, while the resolution is, coincidentally, 4% FWHM.

(2) This table includes all data from situations when the beam magnets were actually tuned for maximum flux. Many of these are not production runs.

TABLE Vb

DATA RUN MOMENTA (GeV/c)

| MOMENTUM (Nominal) | BNL Tape | ANALOG Track | DVM READINGS $D_2$ | DVM READINGS $D_1$ | DVM READINGS $Q_5Q_6$ | CORRECTED MOMENTUM[1] From $D_2$ | CORRECTED MOMENTUM[1] From $D_1$ | CORRECTED MOMENTUM[1] Combined Value |
|---|---|---|---|---|---|---|---|---|
| | | | PRELIMINARY RUNS | | | | | |
| 10 | 1 | 4,7 | 29.4 | 25.1 | 21.0 | 9.2 | -- | ($Q_2$ on at 49.0) |
| 20 | 2 | 1 | 48.4 | 49. | 34.7 | 15.0 | 15.5 | 15.25 |
| 20 | 2 | 4,7 | 57.5 | 59.0 | 39.0 | 17.8 | -- | ($Q_2$ on at 49.1) |
| 15 | 3 | 1 | 44.0 | 42.5 | 32.8 | 13.6 | 13.6 | 13.6 |
| 20 | 3 | 4 | 57.5 | 59.0 | 35 | -- | 17.8 | ($D_1$ not tuned) |
| 15 | 3 | 7 | 44.2 | 42.5 | 32.8 | -- | 13.6 | ($D_1$ not tuned) |
| | | | PRODUCTION RUNS | | | | | |
| 15 | 4 | 1,4 | 44.3 | 43.7 | 37.1 | 13.7 | 14.0 | 13.85 |
| 20 | 4 | 7 | 57.5 | 59.0 | 37.1 | -- | 17.8 | ($D_1$ not tuned) |
| 10 | 5 | 1 | 29.4 | 29.8 | 21.0 | 9.2 | 9.65 | 9.4 |
| 20 | 5 | 4 | 57.5 | 47.6 | 37.6 | -- | -- | -- (1600 events) |
| | | | | | off | 17.8 | 17.0 | 17.4(6000 events) |
| 10 | 5 | 7 | 29.4 | 29.0 | 26.5 | 9.2 | 9.4 | 9.3 |
| 10 | 6 | 1,4,7 | 29.4 | 29.0 | 26.5 | 9.2 | 9.4 | 9.3 |
| 10 | 7 | 1,4,7 | 29.4 | 29.0 | 26.5 | 9.2 | 9.4 | 9.3 |
| 20 | 8 | 1 | 57.5 | 48.5 | 38.1 | -- | -- | -- |
| | | | | | off | 17.8 | 17.4 | 17.6 after $Q_{56}$ off |
| 20 | 8 | 4,7 | 57.5 | 57.5 | 36.1 | 17.8 | 17.5 | 17.65 |
| 20 | 9 | 1,4 | 57.5 | 57.5 | 36.1 | 17.8 | 17.5 | 17.65 |
| 20 | 9 | 7 | 57.5 | 48.5 | off | 17.8 | 17.4 | 17.6 |
| 20 | 10 | 1,4,7 | 57.5 | 57.5 | 37.0 | 17.8 | 17.5 | 17.65 |
| 20 | 11 | 1,4 | 57.5 | 57.5 | 37.0 | 17.8 | 17.5 | 17.65 |

(1) The momentum calculation is described in the test. The best estimate of the central value is the combined value, where listed. This is known to about $\pm$ 4%, while the resulution is, coincidentally, 4% FWHM.

LIST OF FIGURES

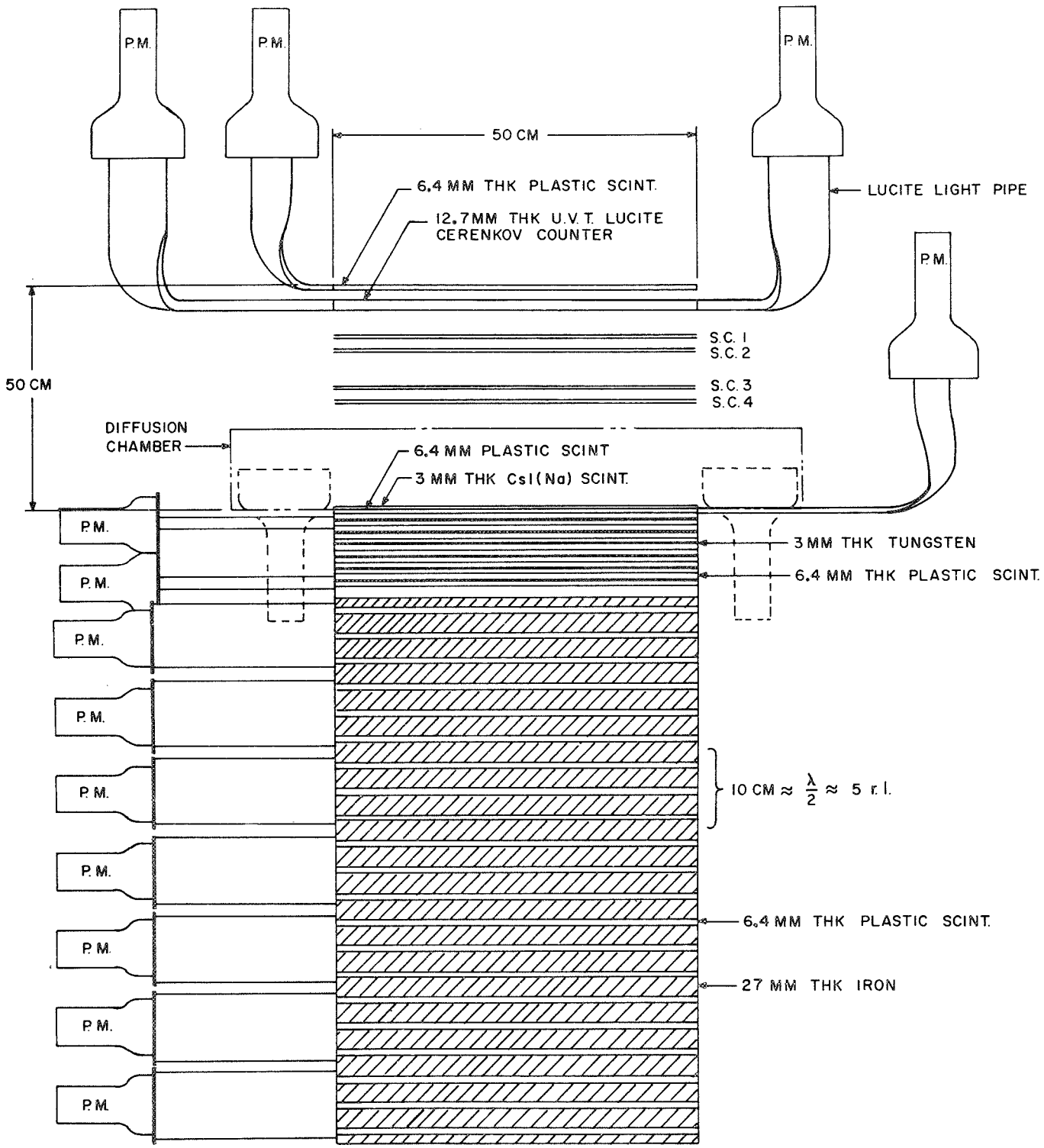


FIGURE 1

SCHEMATIC CROSS SECTION OF
HIGH ENERGY COSMIC RAY EXPERIMENT

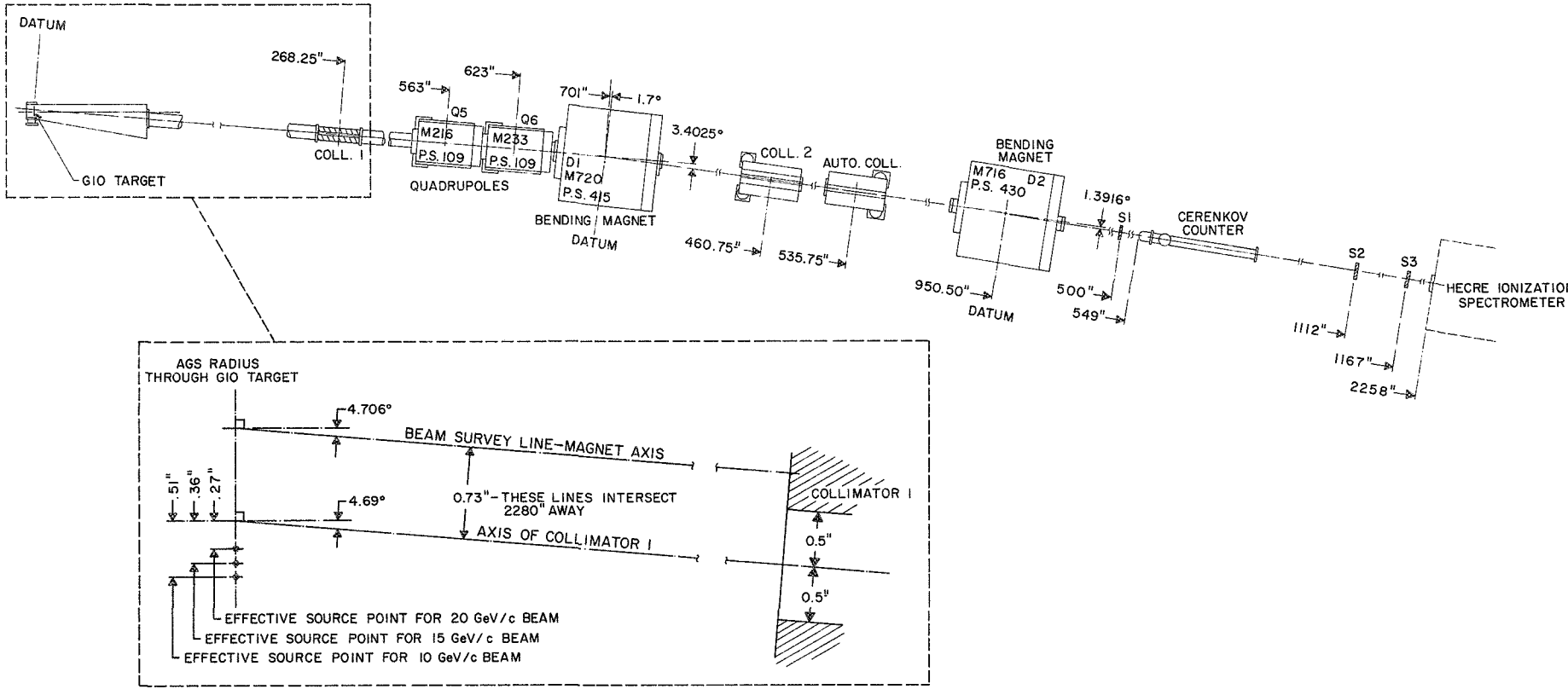


FIGURE 2

SCHEMATIC OF G-10 +4.7° TEST BEAM
TRANSPORT SYSTEM 18-21 JULY 1970

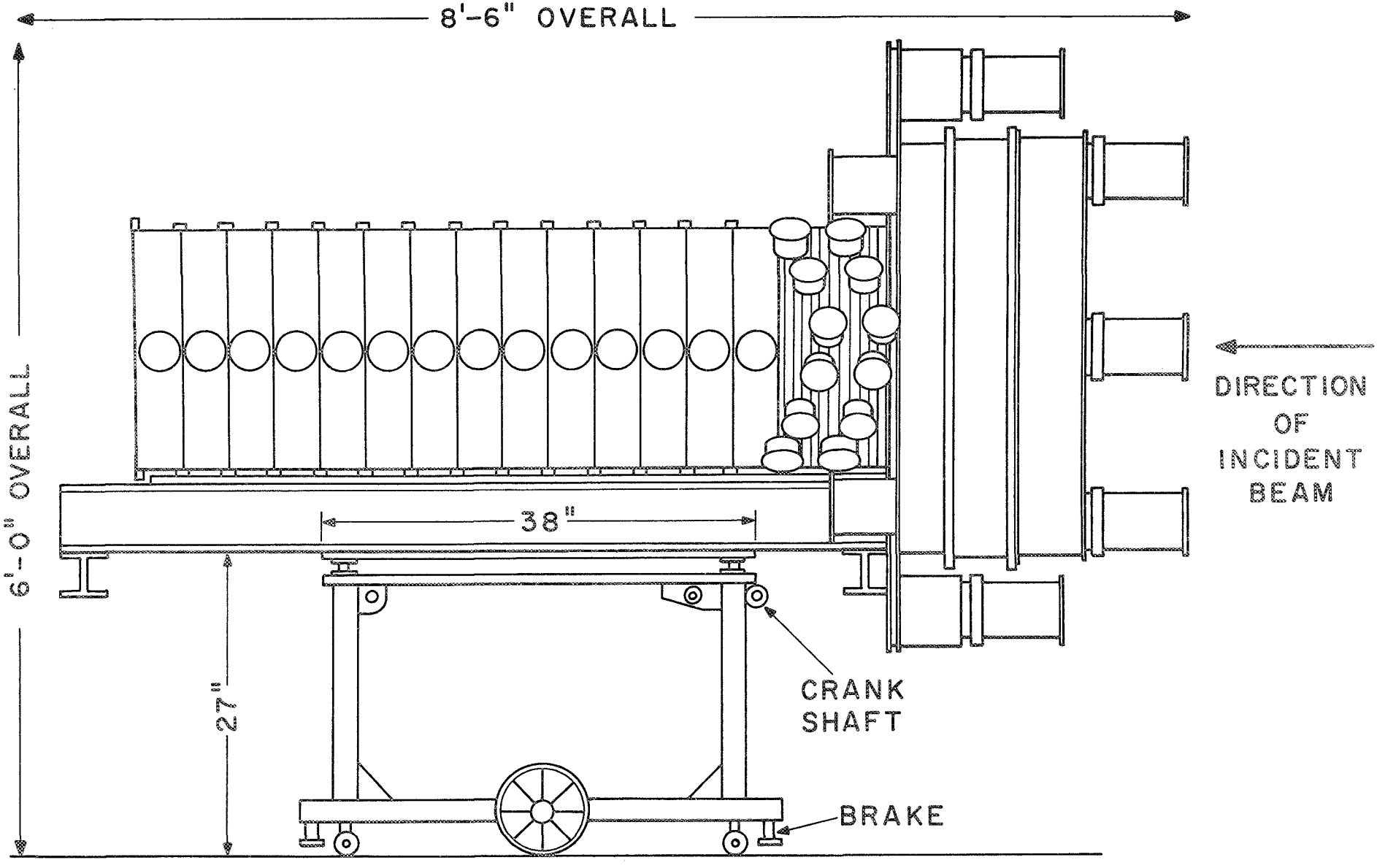


HECRE TEST MOUNTED

FIGURE 3

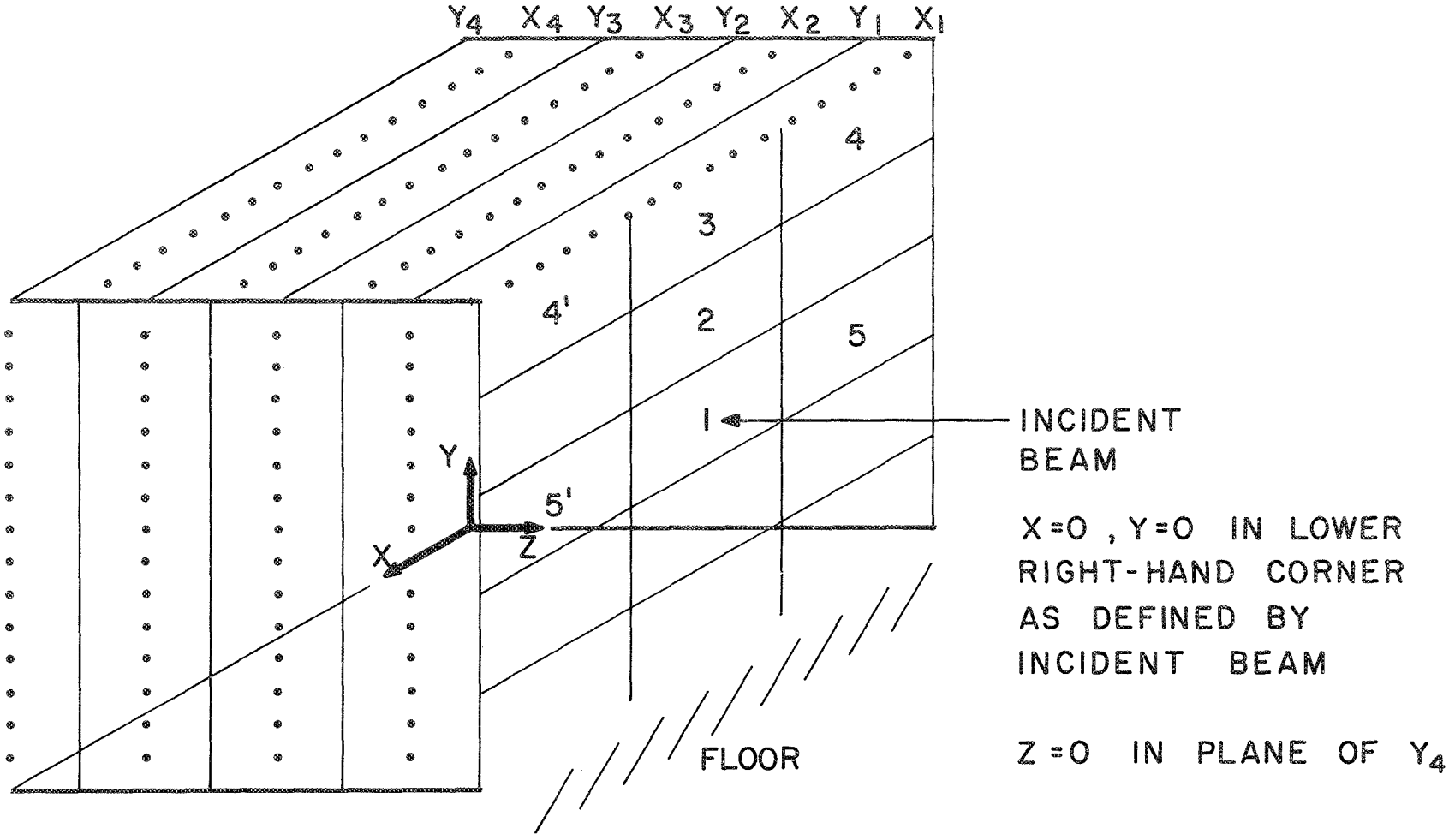


FIGURE 4

SPARK CHAMBER ORIENTATION WITH RESPECT TO INCIDENT BEAM DURING BNL CALIBRATION